

Absorptance of PbS quantum dots thin film deposited on trilayer MoS₂

Bablu Mukherjee¹, Asim Guchhait², Yinthal Chan², Ergun Simsek^{1*}

¹Department of Electrical and Computer Engineering, School of Engineering and Applied Science, The George Washington University, Washington, D.C. 20052, USA

²Department of Chemistry, National University of Singapore, 3 Science Drive 3, 117543, Singapore

*Corresponding author. E-mail: simsek@gwu.edu

Received: 12 June 2015, Revised: 26 August 2015 and Accepted: 30 August 2015

ABSTRACT

We have studied the optical absorptance of lead sulfide (PbS) quantum dot (QD) coated thin crystalline layered material (TCLM) experimentally and numerically. Starting with the synthesis, fabrication and characterizations, a sample of PbS QDs deposited on trilayer molybdenum disulphide (MoS₂) thin film has been probed locally using a reflection spectrometer set-up. Since transmittance is needed to calculate the absorptance of the QD film/TCLM sample, we run a set of simulations using a 3D finite-difference time-domain full-wave electromagnetic solver. Based on the agreement between experimental and numerical results for the reflectance spectra, which verifies the accuracy of our QD and TCLM modelling, we have calculated the absorptance. Unlike metal nanoparticle decorated TCLMs in which metal nanoparticles act like induced dipoles and enhance the absorptance, here we have not observed the similar effect; rather we have found that the absorptance of QD film/TCLM sample is almost equal to the summation of QDs' and TCLM's individual absorptance in the wavelength range of 450-800 nm. Copyright © 2015 VBRI Press.

Keywords: Quantum dots; PbS; MoS₂; TMDC; absorption.

Introduction

Nanocrystalline semiconducting quantum dots (QDs) are promising materials for light absorption, which has been implemented in many applications including planar thin-film based solar cells [1]. Two dimensional (2D) thin crystalline layered materials (TCLMs) such as molybdenum disulphide (MoS₂) attribute good optical absorption in visible wavelength range [2-6]. Integrating these two materials of two different morphological structures into a composite material of 2D-0D system actively, one could engineer the optical absorption of the material [7, 8]. Van der waals heterojunctions of atomically thin transitional metal dichalcogenides (TMDCs) have been proven to be attractive candidates for solar energy conversion [2, 4]. 2D layered crystals of MoS₂ and zero dimension (0D) QD structures of lead sulfide (PbS) are well-known with direct optical band-gap of ~1.6-1.8 and ~1.3-1.4 eV, respectively, and hence MoS₂-PbS hybrid materials hold a great for next generation optoelectronic device applications [8].

Thin-film absorbers based on heterojunctions offer a potential role in photovoltaics for solar harnessing applications [9]. It captures a great area of research interest of using thinner active single crystalline layers combined with advanced light trapping materials to maximize the optical absorption efficiency of the hybrid material by reducing the active volume. Extremely thin and highly dispersive nature of mono- and a few layers of TMDCs

makes them even more attractive for energy harvesting applications. They have extremely high excitonic absorption efficiency (~30 %) in the lower portion of the visible range. However, their average absorption over the entire visible range is quite low (~8 %). Thus decorating these thin crystalline TMDCs with nanoparticles [10-12] or nanocrystalline QDs may enhance their optical absorptance [8]. A previous report describes the use of PbS QDs on top of monolayer MoS₂ to enhance the photosensing efficiency of the detector for $\lambda > 650$ nm, where highly sensitive hybrid material based device benefits from the interaction of 2D MoS₂ and 0D QDs.

In this report, we fabricate as-synthesized PbS QD thin films on top of tri-layer (3L) MoS₂ supported by SiO₂/Si substrate, where SiO₂ layer is ~300 nm thick. The physical properties of the fabricated samples are determined using Transmission Electron Microscopy (TEM), Scanning Electron Microscopy (SEM), Atomic Force Microscope (AFM), and Raman spectroscopy. Their optical properties are characterized using a home-built reflection spectroscopy set-up and commercially available full wave electromagnetic finite-difference time-domain (FDTD) simulation software, Lumerical [13]. Based on the agreement between experimental and numerical reflectance results, we calculate the absorptance spectrum of QD film coated MoS₂ samples using simulation results. We conclude that the average absorptance of PbS QDs/MoS₂

film is almost equal to the linear summation of individual average absorbances of PbS QD film and 3L MoS₂ in wavelength range of 450 to 800 nm. In other words, we do not observe any enhancement in optical absorbance of the hybrid material.

Experimental

Material synthesis

PbS QDs are synthesized as follows. Lead oxide (PbO), oleic acid (OA), bis(trimethylsilyl)sulfide (TMS) are purchased from Sigma Aldrich. All the chemicals are used as received without further purification. Unless stated otherwise, all reactions are conducted in oven-dried glassware under nitrogen atmosphere using standard Schlenk techniques. PbS nanocrystals are synthesized by following a reported procedure [14]. At first, 446 mg (2 mmol) PbO is dissolved in a mixture of 1.5 mL oleic acid and 18.5 mL octadecene. When the mixed solution is heated to 150 °C for ~1 h under nitrogen environment, lead oleate formed. Then temperature of the solution is lowered to ~80 °C. A mixture of 0.2 mL of TMS and 5 mL of octadecene (ODE) are rapidly injected into the lead oleate solution under vigorously stirring condition. The rapid injection of the solution into the reaction flask set-up changes the color of the reaction mixture from colorless to deep brown indicating the formation of nanocrystals. The reaction continued for ~2 minutes so that PbS nanocrystals are formed. Grown nanocrystals are isolated by precipitation with methanol and acetone, followed by centrifugation at 4000 rpm (25 °C). The nanocrystals in QDs morphology are re-dispersed in toluene and the isolation process is repeated for two more times to remove the un-reactants. To obtain QDs with particular diameter, we optimize the amount of oleic acid and octadecene by keeping the total concentration of the precursor same.

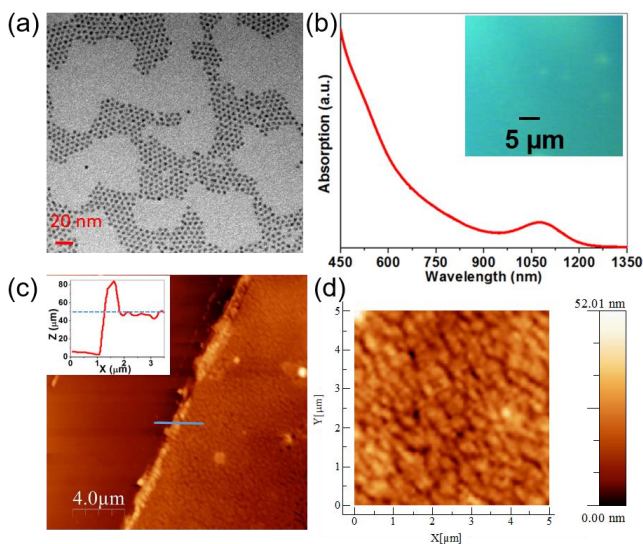


Fig. 1. (a) TEM image of the as-synthesized PbS QDs. (b) Absorption spectrum of the solution based QDs. Inset shows the optical image of the QD thin film. (c) QD thin film fabrication on top of SiO₂/Si substrate. Inset shows the line profile of the thickness across the line shown in (c). (d) Surface topography image of the PbS thin film.

Characterizations

A JEOL JEM 1220F (100 kV accelerating voltage) microscope is used to obtain bright field TEM image of the as synthesized QDs. For TEM sample preparation, a drop of the prepared QD solution is placed onto a 300 mesh copper grid covered with a continuous carbon film. Excess solution is removed by an adsorbent paper and the sample is dried at room temperature. For solution based sample, absorption spectrum is obtained with Shimadzu UV-VIS-NIR UV-3600 spectrophotometer using a quartz cuvette with a path length of ~1 cm. We record the AFM data via a Bruker Dimension FastScan AFM operating in tapping mode (FASTSCAN-A) and “Nanoscope Analysis” software is used to determine the height profile of the nanoparticle-like structures based thin film by making a scratch on the continuous film, which is deposited onto the SiO₂/Si substrates. A confocal Raman microscopic system (Horiba Jobin-Yvon LabRam) and the Raith 150 system for SEM (operating at 5 kV accelerating voltage) image are used to characterize the fabricated samples. A home-built optical setup is used to measure the reflectance as explained in the next section.

Results and discussion

Fig. 1(a) shows the topological characterization of PbS QDs by TEM imaging. One can note that the PbS QDs are uniform and mono-dispersed. Analysis of TEM image (**Fig. 1(a)**) reveals that the average sizes of the QDs are ~ 5.5 nm. The optical absorption spectrum of the PbS QDs dispersed in toluene has a small hump feature at around 1075 nm, with a broad excitation profile that extends across the NIR spectral window, as shown in **Fig. 1(b)**. Thin films of close-packed PbS QDs on SiO₂/Si substrate are prepared by spin casting for solid state film based measurements as shown by the optical image in the inset of **Fig. 1(b)**. As synthesized PbS QD solution in toluene media with a concentration of 90 mg/mL is spin-coated at 2000 rpm for 30 seconds and baked for 5 minutes on a hotplate at substrate temperature of 80 °C at air atmosphere. Uniform solid thin film of PbS QDs on SiO₂/Si substrate is shown by the AFM image (**Fig. 1(c)**), which is obtained in a large area. The film thickness is estimated to be ~ 45 nm as shown in the line profile inset in **Fig. 1(c)**. The quality of surface morphology and homogeneities of the solid film formation are examined via the surface topography imaging (**Fig. 1(d)**), which indicates that the average roughness of the QD film is ~ 5.7 nm. As prepared PbS QD thin films are used for measurements without doing any further chemical treatments. It can be noted that various phenomena like dielectric environment changes, and/or inter-QD wave function overlapping by making a nonradiative coupling, can occur when the solvent is removed from the QD solution to form solid thin film, which may modulate the optical properties of the film.

Few layer MoS₂ nanosheets (thickness ≥ 3 layers) are micromechanically exfoliated using a piece of adhesive scotch tape from commercially available bulk MoS₂ bulk crystals (2D Semiconductors Inc. supplies) on top of n-doped silicon substrate with coating oxide of ~300 nm thickness. Optical image of the fabricated MoS₂ sample is shown in the inset of **Fig. 2(a)**. The thickness and sample quality are characterized using a confocal Raman

microscopy system, where the spectrum is collected by a 100x objective lens in a backscattering geometry as shown in **Fig. 2(a)**. A small hump at $\sim 450 \text{ cm}^{-1}$ and a high intense peak at $\sim 520.5 \text{ cm}^{-1}$ are known to be arising from background substrate corresponding to SiO_2 layer and crystalline Si substrate, respectively. The other two Raman peaks in the spectrum at ~ 383.3 and $\sim 407.2 \text{ cm}^{-1}$ are matching with the reported Raman vibrational modes E_{2g}^1 and A_{1g} , respectively, of few layer thick MoS_2 film on SiO_2/Si substrate, which also confirms the chemical purity of the sample. By looking at the frequency difference of the E_{2g}^1 and A_{1g} Raman modes, which is $\sim 23.9 \text{ cm}^{-1}$, the thickness of the MoS_2 film can be quantified to be trilayer (3L) thick [15]. Suspending PbS QD sample in toluene media, which are capped with oleate-ligand is then spin-coated (SCS 6800 Spin Coater Series) over the MoS_2 thin film supported by $\text{SiO}_2(300 \text{ nm})/\text{Si}$ substrate and the thickness of the film is estimated to be around 45 nm thick. A schematic representation of one layer of PbS QD coating on thin MoS_2 layer on top of SiO_2/Si substrate is shown in **Fig. 2(b)** to demonstrate the anchoring process of QDs on MoS_2 surface. After coating with QDs, the substrate is placed on hot plate at substrate temperature of $\sim 80 \text{ }^\circ\text{C}$ for ~ 5 minutes. SEM and optical microscopy (OM) images of the thin PbS QD film coated MoS_2 flakes grown by chemical vapor deposition (CVD) techniques [16] are shown in **Fig. 2(c)** (inset) and **Fig. 2(d)**, respectively.

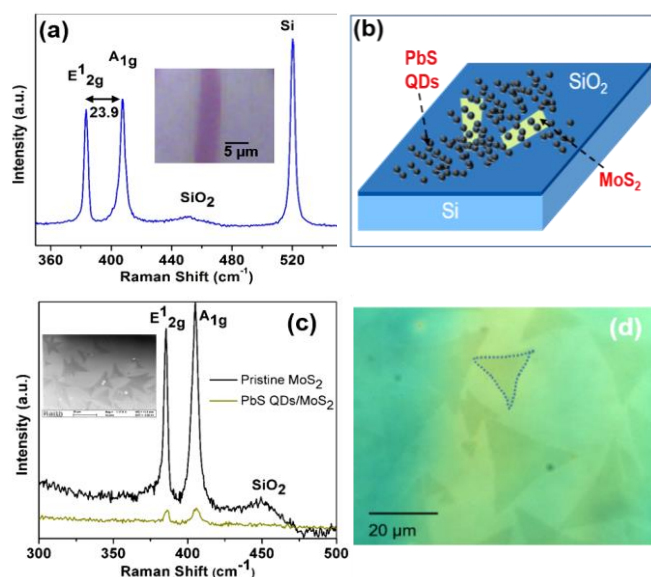


Fig. 2. (a) Raman spectrum (532 nm laser excitation) of the thin MoS_2 layer sample formed on top of SiO_2/Si substrate. (b) Schematic diagram of PbS QD coated few layer MoS_2 on SiO_2/Si substrate. (c) Raman spectra of pristine MoS_2 sample with and without PbS QD film coating. Inset shows SEM image of the PbS QD film coated MoS_2 sample and (d) Optical microscopy image of PbS QD film coated MoS_2 sample on SiO_2/Si substrate. One crystalline flake is shown by dotted line.

Thin MoS_2 crystalline flakes are still visible in both SEM and OM images even after coating with thin QD film. After PbS QD coating on top of the exfoliated $\text{MoS}_2/\text{SiO}_2/\text{Si}$, it has observed (**Fig. 2(c)**) that the main two vibrational modes of pristine MoS_2 in Raman spectrum match with the main Raman vibrational modes of the hybrid (PbS/ MoS_2) sample indicating the preserved signature of the crystalline MoS_2 sample.

Various thin MoS_2 samples obtained from CVD growth and mechanically exfoliation techniques are characterized with and without QD coating using non-contact reflection probe measurements technique [17] with a setup similar to the one depicted in **Fig. 3**.

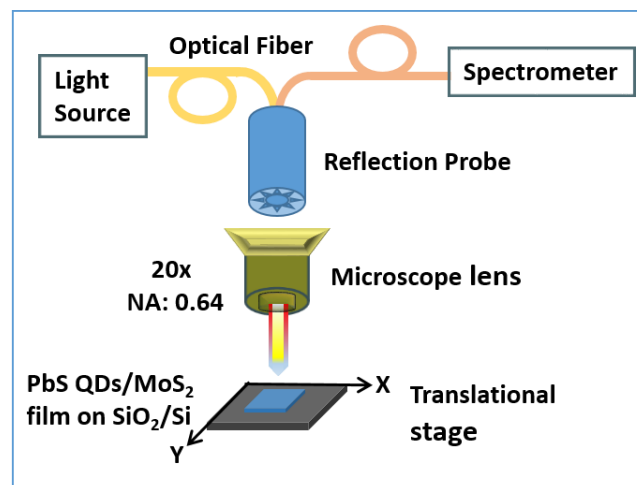


Fig. 3. Schematic diagram of reflection probe based optical measurements set-up.

Here, we use a white light source (a Halogen lamp), which is coupled into an optical fiber of premium-grade reflection probe (Ocean Optics). Then the light passes through a 20x objective lens (NA: 0.64) to illuminate the sample, which is kept at focal plane of the objective lens [11, 16]. The detail of the locally probed reflection spectrometry is previously published by our group [11]. The light reflected from the sample is directed towards objective lens and then collected by reflection probe (at the same angle as it illuminates) to analyze by the spectrometer (USB 4000 Ocean Optics). Reflection spectra of the fabricated PbS thin film, 3L thick MoS_2 film, and PbS QD coated 3L MoS_2 film (PbS/ MoS_2 film) samples on top of SiO_2/Si substrate are experimentally recorded in the wavelength range of 450 to 800 nm as shown in **Fig. 4(a)**. The PbS film has a good optical reflection peak at ~ 580 nm, and the optical reflection covers the wavelength region of ~ 420 to ~ 720 nm, consistent with the previously reported findings [18]. There are two excitonic peaks in reflection spectra observed for the 3L MoS_2 film located at ~ 621 nm and ~ 671 nm, which corresponds to the MoS_2 'B' and 'A' peaks, respectively. Whereas PbS QDs/ MoS_2 sample shows a similar shaped reflection spectrum with 3L MoS_2 sample with bit more prominent excitonic peak intensities.

Experimentally obtained reflection spectra are further analysed with the simulation results. A commercial-grade simulator based on the finite-difference time-domain (FDTD) method is used to perform the calculations [13]. Plane wave is used as source in the unit cell to simulate the reflection spectra (R), which is recorded in a monitor placed behind the excitation source (R_{port}) as shown in the schematic of unit cell diagram inset in **Fig. 4(b)**. In order to obtain more realistic results, we use wavelength-dependent refractive index formulas for each material. The refractive indices of MoS_2 from [19], SiO_2/Si from [20], and PbS from [21] are used in the simulation. The thickness of MoS_2 is assumed to be 2.1 nm (equivalent to 3L thickness),

whereas thin film of spherical PbS QDs (diameter 5 nm) is assumed to be 55 nm thick with inter QD separation of ~ 2 nm (edge to edge separation) along the x -axis by making high QD packing density. In order to obtain highly accurate results, a very fine meshing is applied, where mesh sizes are set to 0.1 nm along MoS₂, 0.5 nm along PbS film, and 2 nm for the rest of the structure. Perfectly matched layer (PML) along z -axis and periodic boundary conditions along x - and y -axis are used in the simulation unit. The recorded reflection spectra are multiplied with the Gaussian beam profile of halogen bulb source (spectrum of HL-2000 family tungsten halogen light sources for the Vis-NIR, Ocean Optics), which is used in the experiment, to mimic the experimentally measured data. Three different configurations of geometry i.e. PbS QD film, few layer MoS₂ film and QD coated MoS₂ film on SiO₂/Si substrate are considered similar with experiments and the estimated reflection spectra from simulation results are plotted in Fig. 4(b). Fig. 4 (a), which is experimentally, obtained results, matches very well with the simulated reflection spectra results in Fig. 4(b), which validates the accuracy of our FDTD modelling with QDs and MoS₂ thin film. Various defect states, which may associate with as-synthesized QDs, inter-QD coupling of higher excitonic states, scattering phenomena from thin film inhomogeneities of experimental results, are neglected in the simulation model.

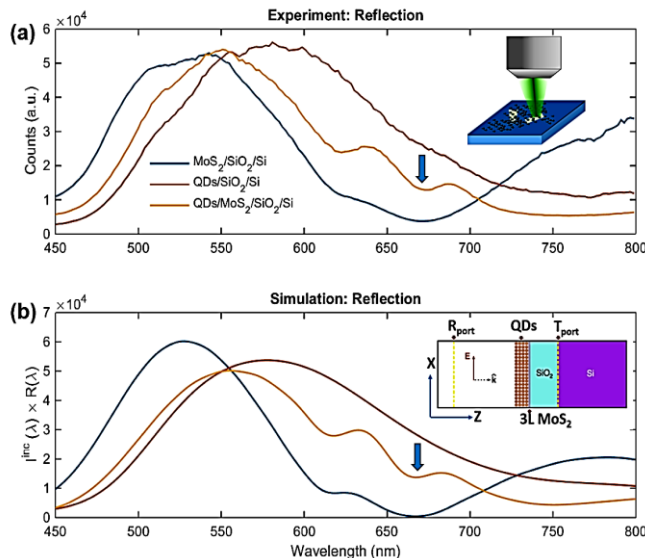


Fig. 4. (a) Reflection spectra of few layer MoS₂ sample with and without coated with PbS QD film formed on top of SiO₂/Si substrate and spectrum of PbS QD thin film coated SiO₂/Si substrate. Inset shows the schematic diagram of the localized reflection measurement technique and (b) Simulated reflection spectra. Inset shows the schematic representation of unit cell of the simulation set-up. 'A' excitonic peak position is marked by arrow in both figures.

As we study the average absorption by few layers MoS₂ covered with thin film of PbS QDs, we need to exclude the optical absorption of the thick Si substrate. Experimentally if we want to calculate absorption spectra of the fabricated hybrid material, which occur only due to active material PbS/MoS₂ then it is merely difficulty to remove the optical absorption of thick Si substrate. Thus if we need to evaluate the absorbance of the individual material then we need to simulate the spectra as mentioned follows. Here in the

second part of the simulation, where we use T_{port} (see inset diagram in Fig. 4(b)) to record transmission spectra (T) by placing a secondary port at the interface plane between Si substrate and SiO₂ layer. Considering the fact that the PML layers do not reflect anything back, T_{port} indeed records the transmittance of PbS/MoS₂ region only. Absorption spectra (A) are calculated using the relation, which is equal to "1 - Reflection - Transmission". The recorded R, T spectra and calculated absorption (A) are plotted in Fig. 5(a, b, and c), which are corresponding to 3L MoS₂, thin PbS QD film and PbS/MoS₂ film, respectively.

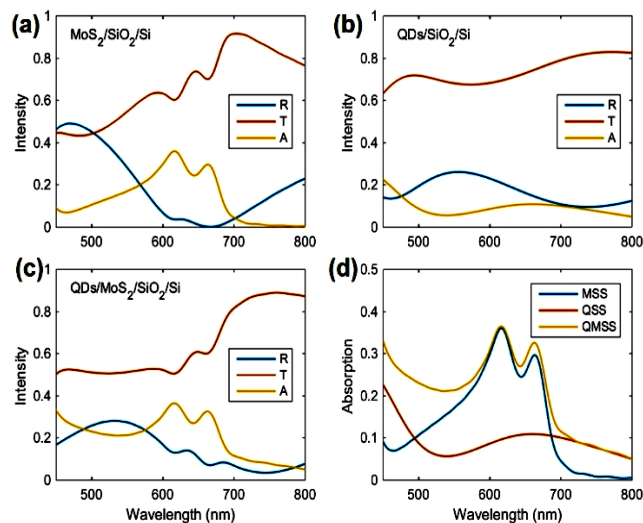


Fig. 5. (a, b, and c) Simulated reflection (R), transmission (T) and absorption (A) spectra of MoS₂(3L)/SiO₂/Si (MSS), QD film/SiO₂/Si (QSS), and QD coated 3L MoS₂/SiO₂/Si (QMSS), respectively and (d) Absorption spectra of the films.

For comparison purpose, all three absorption spectra are plotted in the same Fig. 5(d), which infers that the average absorption in PbS/MoS₂ composite material is almost equal to sum of individual film's average absorption. Hence the overall average absorption of 3L MoS₂, thin film of PbS sample, and PbS QD film coated MoS₂ sample are ~ 14.36 %, 9.8 %, and ~ 22.37 %, respectively, in the wavelength range of 450-800 nm. Thus it can be infer that the average optical absorption of the PbS/MoS₂ sample is also almost equal to sum of the average absorptions of PbS film and trilayer MoS₂. Considering the non-linear emission spectra of quantum dots, there may have a non-linear enhancement but the phenomena is not observed due to its weakness compared to the excitation. From the physical point of view, this result first confirms that the method used for QD decoration (precipitation with methanol and acetone, centrifugation at 4000 rpm, re-dispersion in toluene) indeed removes the un-reactants (otherwise we would not observe such a linear response); second, it shows that the polarizability of PbS QDs in the visible is weak so that the secondary field (created by the induced PbS QDs) is almost negligible compared to field absorbed by and scattered from the QDs.

To have a better physical understanding of our experimental results, we calculate the absorption (σ_{abs}) and scattering (σ_{sca}) cross section of PbS quantum dots using Mie theory [22]. A PbS QD with a diameter of 5.5 nm is assumed to be placed on top of a multilayered substrate

(trilayer MoS₂/ 300 nm SiO₂/ Si). Again, all the materials are defined using their wavelength dependent refractive indices. Our calculations show that σ_{abs} of PbS QDs is always much higher than σ_{sca} for example at the wavelength of 600 nm, $\sigma_{\text{abs}} \approx 20000 \times \sigma_{\text{sca}}$. This means that scattered field is 4 orders of magnitude smaller than the absorbed field. Considering how fast electric field decays with distance, there is no doubt that QDs which are made of very lossy material and extremely small compared to wavelength cannot create an enhancement in the overall absorption of the hybrid structure.

Conclusion

In summary, we have studied the optical absorbance of quantum dot coated thin crystalline transition metal dichalcogenide films experimentally and numerically. Fabrication and characterization of 3L MoS₂ coated with PbS QD thin film samples are investigated. Even though the absorbance of these films is higher and broader than quantum dots' and TMDC films' individual absorbances, we do not observe any enhancement in optical absorbance of the hybrid material. In other words, the overall absorbance of QD coated TMDC films is almost equal to the sum of quantum dots' and TMDC films' individual absorbances in wavelength range of 450-800 nm.

Reference

- Kamat, P. V.; *J. Phys. Chem. Lett.*, **2013**, *4*, 6, 908.
DOI: [10.1021/jz400052c](https://doi.org/10.1021/jz400052c)
- Furchi, M. M.; Pospischil, A.; Libisch, F.; Burgdörfer, J.; Mueller, T.; *Nano Lett.*, **2014**, *14*, 8, 4785.
DOI: [10.1021/nl501962c](https://doi.org/10.1021/nl501962c)
- Bernardi, M.; Palumbo, M.; Grossman, J. C.; *Nano Lett.*, **2013**, *13*, 3664.
DOI: [10.1021/nl401544y](https://doi.org/10.1021/nl401544y)
- Song, X.; Hu J.; Zeng, H.; *J. Mater. Chem. C*, **2013**, *1*, 2952.
DOI: [10.1039/C3TC00710C](https://doi.org/10.1039/C3TC00710C)
- Ye, M.; Winslow, D.; Zhang, D.; Pandey R.; Yap, Y. K.; *Photonics*, **2015**, *2*, 288.
DOI: [10.3390/photonics2010288](https://doi.org/10.3390/photonics2010288)
- Li, W.; Birdwell, A. G.; Amani, M.; Burke, R. A.; Ling, X.; Lee, Y. H.; Liang, X.; Peng, L.; Richter, C. A.; Kong, J.; Gundlach, D. J.; Nguyen, N. V.; *Phys. Rev. B*, **2014**, *90*, 195434.
DOI: [10.1103/PhysRevB.90.195434](https://doi.org/10.1103/PhysRevB.90.195434)
- Prasai, D.; Klots, A. R.; Newaz, A. K. M.; Niezgod, J. S.; Orfield, N. J.; Escobar, C. A.; Wynn, A.; Efimov, A.; Jennings, G. K.; Rosenthal, S. J.; Bolotin, K. I.; *Nano Lett.*, **2015**, *15*, 7, 4374.
DOI: [10.1021/acs.nanolett.5b00514](https://doi.org/10.1021/acs.nanolett.5b00514)
- Kufer, D.; Nikitskiy, I.; Lasanta, T.; Navickaite, G.; Koppens, F. H. L.; Konstantatos, G.; *Adv. Mater.*, **2015**.
DOI: [10.1002/adma.201402471](https://doi.org/10.1002/adma.201402471)
- Gu, W.; Yang, F.; Wu, C.; Zhang, Y.; Shi, M.; Ma, X.; *Nanos. Res. Lett.*, **2014**, *9*, 662.
DOI: [10.1186/1556-276X-9-662](https://doi.org/10.1186/1556-276X-9-662)
- Mukherjee, B.; Leong, W. S.; Li, Y.; Gong, H.; Sun, L.; Shen, Z. X.; Simsek, E.; Thong, J. T. L.; *Mater. Res. Exp.*, **2015**, *2*, 065009.
DOI: [10.1088/2053-1591/2/6/065009](https://doi.org/10.1088/2053-1591/2/6/065009)
- Mukherjee B.; Simsek, E.; Plasmonics Enhanced Average Broadband Absorption of Monolayer MoS₂, *Plasmonics*, **2015**, *11*, 1.
DOI: [10.1007/s11468-015-0053-9](https://doi.org/10.1007/s11468-015-0053-9)
- Simsek, E.; *Plasmonics*, **2009**, *4*, 3, 223.
DOI: [10.1007/s11468-009-9096-0](https://doi.org/10.1007/s11468-009-9096-0)
- Lumerical Solutions, Inc. www.lumerical.com/tcad-products/fdtd/
- Ratanatawanate, C.; Tao, Y.; Balkus, K. J.; *J. Phys. Chem. C*, **2009**, *113*, 10755.
DOI: [10.1021/jp903050h](https://doi.org/10.1021/jp903050h)
- Lee, C.; Yan, H.; Brus, L. E.; Heinz, T. F.; Hone, J.; Ryu, S.; *ACS Nano*, **2010**, *4*, 5, 2695.
DOI: [10.1021/nn1003937](https://doi.org/10.1021/nn1003937)

- Mukherjee, B.; Tseng, F.; Gunlycke, D.; Amara, K. K.; Eda, G.; Simsek, E.; *Opt. Mat. Exp.*, **2015**, *5*, 2, 447.
DOI: [10.1364/OME.5.000447](https://doi.org/10.1364/OME.5.000447)
- Luther, J. M.; Law, M.; Song, Q.; Perkins, C. L.; Beard, M. C.; Nozik, A. J.; *ACS Nano*, **2008**, *2*, 2, 271.
DOI: [10.1021/nl7003348](https://doi.org/10.1021/nl7003348)
- Zhang J.; Jiang, X.; *Appl. Phys. Lett.*, **2008**, *92*, 141108.
DOI: [10.1063/1.2907492](https://doi.org/10.1063/1.2907492)
- Li, Y.; Chernikov, A.; Zhang, X.; Rigosi, A.; Hill, H. M.; Van der Zande, A. M.; Chenet, D. A.; Shih, E. M.; Hone, J.; Heinz, T. F.; *Phys. Rev. B*, **2014**, *90*, 205422.
DOI: [10.1103/PhysRevB.90.205422](https://doi.org/10.1103/PhysRevB.90.205422)
- Rakić, D.; Djurišić, A. B.; Elazar, J. M.; Majewski, M. L.; *Appl. Opt.*, **1998**, *37*, 5271.
DOI: [10.1364/AO.37.005271](https://doi.org/10.1364/AO.37.005271)
- Moreels, I.; Kruschke, D.; Glas, P.; Tomm, J. W.; *Opt. Mat. Exp.*, **2012**, *2*(5), 496.
DOI: [10.1364/OME.2.000496](https://doi.org/10.1364/OME.2.000496)
- Simsek, E.; *Opt. Express* **2010**, *18*, 1772.
DOI: [10.1364/OE.15.017482](https://doi.org/10.1364/OE.15.017482)

Advanced Materials Letters

Copyright © VBRI Press AB, Sweden
www.vbripress.com

Publish your article in this journal

Advanced Materials Letters is an official international journal of International Association of Advanced Materials (IAAM, www.iaamonline.org) published by VBRI Press AB, Sweden monthly. The journal is intended to provide top-quality peer-review articles in the fascinating field of materials science and technology particularly in the area of structure, synthesis and processing, characterisation, advanced-state properties, and application of materials. All published articles are indexed in various databases and are available download for free. The manuscript management system is completely electronic and has fast and fair peer-review process. The journal includes review article, research article, notes, letter to editor and short communications.

